Published in final edited form as:
Oncogene. 2010 June 3; 29(22): 3185–3195. doi:10.1038/onc.2010.75.

Human stem cells expressing novel TSP-1 variant have anti-angiogenic effect on brain tumors

Mark van Eekelen[1,2,7], **Laura Sasportas**[1,2,7], **Randa Kasmieh**[1,2], **Stephen Yip**[4,5], **Jose-Luiz Figueiredo**[2], **David N. Louis**[4,5], **Ralph Weissleder**[2,6], and **Khalid Shah**[1,2,3]

[1]Molecular Neurotherapy and Imaging Laboratory, Massachusetts General Hospital, Harvard Medical School, Boston, Massachusetts

[2]Department of Radiology, Massachusetts General Hospital, Harvard Medical School, Boston, Massachusetts

[3]Department of Neurology, Massachusetts General Hospital, Harvard Medical School, Boston, Massachusetts

[4]Department of Pathology, Massachusetts General Hospital, Harvard Medical School, Boston, Massachusetts

[5]MGH-Cancer Center, Massachusetts General Hospital, Harvard Medical School, Boston, Massachusetts

[6]Center for Systems Biology, Massachusetts General Hospital, Harvard Medical School, Boston, Massachusetts

Abstract

Novel therapeutic agents combined with innovative modes of delivery and non-invasive imaging of drug delivery, pharmacokinetics and efficacy are crucial in developing effective clinical anti-cancer therapies. In this study, we have created and characterized multiple novel variants of anti-angiogenic protein thrombospondin (aaTSP-1) that were comprised of unique regions of 3 type-I-repeats of TSP-1 and employed engineered human neural stem cells (hNSC) to provide sustained on-site delivery of secretable aaTSP-1 to tumor-vasculature. We show that hNSC-aaTSP-1 has anti-angiogenic effect on human brain and dermal microvascular endothelial cells co-cultured with established glioma cells and CD133+ glioma-initiating-cells. Using human glioma cells and hNSC engineered with different combinations of fluorescent and bioluminescent marker proteins and employing bioluminescence imaging and intravital-scanning microscopy, we show that aaTSP-1 targets the vascular-component of gliomas and a single administration of hNSC-aaTSP-1 markedly reduces tumor vessel-density that results in inhibition of tumor-progression and increased survival in mice bearing highly malignant human gliomas. We also show that therapeutic hNSC do not proliferate and remain in an un-differentiated state in the brains of glioma bearing mice. This study provides a platform for accelerated development of future cell based therapies for cancer.

Keywords

‘in vivo imaging’; ‘glioma’; ‘human neural stem cells’; TSP-1’; ‘endothelial cells’; ‘angiogenesis’

Correspondence & reprint requests to: Khalid Shah, Massachusetts General Hospital, Harvard Medical School, kshah@helix.mgh.harvard.edu.

[7]These authors contributed equally to the project

Introduction

Human gliomas, in their proliferative stage, are highly vascularized tumors and their persistence and growth are dependent on the pathological formation of new capillary blood vessels. Angiogenesis inhibition could therefore be an efficient therapeutic strategy for treating malignant gliomas. However, the benefit of current anti-angiogenic agents as standard-alone therapies has been modest. The major limitations in the progress of anti-angiogenic agents to clinics have been their short circulating half life, dose-limiting toxicity and the non-invasive methods to monitor anti-angiogenic therapies *in vivo*. This has prompted the 1) engineering of novel anti-angiogenic agents that can be delivered through innovative modes of delivery; and 2) integration of imaging agents into target cells, delivery vehicles and therapeutic molecules to visualize drug delivery, pharmacokinetics and therapeutic efficacy. Both efforts are aimed at developing effective anti-angiogenic therapies for gliomas.

In recent years, the anti-angiogenic potential of thrombospondin-1 (TSP-1) has been extensively explored. TSP-1 is a 420 kD glycoprotein consisting of a homotrimer containing a NH2-terminal domain, a procollagen domain, type 1, 2 and 3 repeats and a COOH-domain (Lawler & Detmar, 2004). The anti-angiogenic potential of TSP-1 is mainly driven by its three type 1 repeats (TSRs) and a number of studies have shown the anti-angiogenic and anti-tumor effect of TSRs and the peptides originating from TSRs (Anderson et al., 2007; Bogdanov et al., 1999; Lawler & Detmar, 2004; Liu et al., 2003; Rusk et al., 2006). For instance, a therapeutic peptide ABT-510, derived from the GVITRIR sequence in the 2nd TSR of TSP-1, has recently been approved for clinical trial in different cancer types (Hoekstra et al., 2006; Markovic et al., 2007). The short half-life of anti-angiogenic TSP-1 peptides and the inability to non-invasively monitor their pharmacokinetics and efficacy are limitations to the TSP-1 mediated anti-angiogenic therapy. We reasoned that one strategy to overcome these limitations would be to construct a secretable and *in vivo* imageable version of anti-angiogenic (aa) TSP-1, comprising the regions of 3TSRs where most of the peptides used in preclinical and clinical settings have originated from; and employ neural stem cells (NSC) as on-site delivery vehicles to deliver aaTSP-1. We and others have previously shown that both mouse and human NSC migrate towards the tumor site when implanted in the contralateral hemisphere or in the close vicinity of the gliomas (Aboody et al., 2000; Shah et al., 2005; Shah et al., 2008; Tang et al., 2003). This tropism of NSC for brain tumors can be used for delivering therapeutic molecules (Ehtesham et al., 2002; Shah et al., 2005; Shah et al., 2008). In the current study, we have created and characterized multiple secretable variants of anti-angiogenic protein thrombospondin (aaTSP-1) and engineered human NSC with aaTSP-1 to elucidate its anti-angiogenic effects *in vitro* and *in vivo*.

Non-invasive imaging offers a huge potential to facilitate the development of novel cancer therapies. We have previously used dual bioluminescence imaging to follow the fate of neural stem cells (NSC) and tumors *in vivo* (Shah et al., 2005; Tang et al., 2003). However, visualization of multiple biological events in therapeutic tumor models, such as simultaneous monitoring of delivery agents, therapeutic protein secretion, angiogenesis and tumor burden in real-time, has remained largely unexplored so far. In this study, we have also incorporated different combinations of fluorescent and bioluminescent markers into glioma cells and NSC and used real-time optical imaging to simultaneously follow tumor burden, hNSC fate, in situ aaTSP-1 secretion from hNSC and its effects on tumor associated vasculature in a highly malignant human glioma model.

Results

To study the role of secreted anti-angiogenic TSP-1 on human endothelial cells *in vitro* and its effect on glioma angiogenesis and progression in mouse models of glioma tumors, we created different versions of secretable anti-angiogenic TSP-1 (aaTSP-1) encoding the regions of 3TSRs of TSP-1 (a.a. 412–499) where most of the current clinically used anti-angiogenic TSP-1 peptides have originated. The aaTSP-1 plasmid constructs consisting of N-terminal human Flt3 signal sequence (Ss) or the entire extracellular domain of human Flt3 (HF) and also their His_6- and FLAG (Fg) tagged variants to quantify secretion of aaTSP-1 are diagrammed in Fig. 1A. These constructs were packaged into lentivirus (LV) virions and used to transduce human NSC (hNSC) in culture. hNSC were efficiently transduced with aaTSP-1 LVs as revealed by GFP fluorescence (Fig. 1B) and by flow cytometry (Fig. 1C) and expressed aaTSP-1, as shown by dot blot analysis on culture medium (Fig. 1D). In order to quantify secreted aaTSP-1 in the culture medium, we developed an ELISA-assay based on Ni^{2+} -coated wells and biotinylated anti-FLAG antibody. A higher concentration of Ss-aaTSP-1 (240 ng/mL/10^6 cells) compared to HF-aaTSP-1 (160 ng/mL/10^6 cells) protein was secreted in the culture medium (Fig. 1E) of hNSC transduced with different versions of His_6- and FLAG- tagged aaTSP-1 LVs. Furthermore, hNSC continuously secreted aaTSP-1 over a 15 day period (Fig. 1F) and the expression of aaTSP-1 in hNSC did not alter their growth rate (Fig. 1G).

To study the anti-angiogenic effects of different variants of aaTSP-1 *in vitro*, we first measured endothelial cell branch point formation and tubule length, the two most widely used surrogates to estimate angiogenesis *in vitro*, on human microvascular endothelial cells (HMVECs) incubated with conditioned medium from transduced hNSC. HMVECs incubated with Ss-aaTSP-1 containing conditioned medium showed a significant reduction in the formation of branching points (Fig. 2A) and also tubule length (supplementary Fig. 1A), as compared to the HF-aaTSP-1 or control conditioned medium 18 hrs post incubation. There was no influence of N-terminal His and C-terminal FLAG tags on the anti-angiogenic potential of aaTSP-1 (Fig. 2A and 2B). We then tested conditioned medium from hNSC-Ss-aaTSP1 on human brain microvascular endothelial cells (HBMVECs). hNSC-Ss-aaTSP1 significantly inhibited the formation of branching points in HBMVECs (Fig. 2C; supplementary Fig. 1B and 1C). Glioma cells have been reported to secrete factors that promote angiogenesis (Hanahan & Weinberg, 2000; Papetti & Herman, 2002). In order to study the potency of aaTSP1 on endothelial cells in presence of glioma cells, we performed additional co-culture experiments of HMVECs and HBMVECs with either established human glioma cells expressing DsRed2 (Gli36-EGFRvIII-DsRed2) or CD133 positive and negative primary human glioma cells. The conditioned medium from hNSC-Ss-aaTSP-1 caused a reduction in branching points in both HMVECs (Fig. 2D) and HBMVECs (Fig. 2E). HMVECs co-cultured with either CD133+ or CD133− primary glioma cells, and incubated in conditioned medium from hNSC-Ss-aaTSP-1 showed a significant reduction in average branching points (Fig. 2F). Finally, similar studies performed with a known VEGFR2 kinase inhibitor (cell permeable indolin-2-one class of RTK), showed a hNSC-Ss-aaTSP-1 comparable effect on HMVECs (Fig. 2G).These results reveal that neural stem cell secreted aaTSP-1 has anti-angiogenic effect on both HMVECs and HBMVECs *in vitro* and its efficacy is optimized by fusing it to the N-terminal human Flt3 signal sequence (Ss) rather than to the entire extracellular domain of human Flt3 (HF). Furthermore, Ss-aaTSP-1 results in the considerable reduction in the angiogenic potential of endothelial cells when co-cultured with glioma cells and this effect is comparable to the known ant-angiogenic inhibitor used in pre-clinical settings.

In order to follow the secretion of Ss-aaTSP-1 (from here on named aaTSP-1) *in vitro* and *in vivo*, we created a C-terminal *Gaussia* luciferase (Gluc) fusion of aaTSP-1 (Fig. 3A). Gluc is

a naturally secreted bioluminescent protein that has been proven to have enhanced brightness and stability compared to other luciferases and, unlike firefly luciferase (Fluc), does not require ATP for its activity (Verhaegent & Christopoulos, 2002). Branch point formation assays on HMVECs and HBMEVCs revealed that aaTSP-1-Gluc had considerably reduced potency as compared to aa-TSP-1 (data not shown). Gluc bioluminescence imaging on hNSC transduced with LV-aaTSP1-Gluc (Fig. 3B) showed that hNSC secreted aaTSP-1-Gluc in the culture medium (Fig. 3C). In order to simultaneously follow the fate of hNSC and secretion of aaTSP-1, hNSC were co-transduced with LV-aaTSP-1-Gluc and LV-GFP-Fluc and both hNSC and culture medium were imaged using two different substrates, coelenterazine and D-luciferin respectively. Linear correlations between 1) aaTSP1-Gluc activity and culture medium volume; and 2) Fluc activity and the number of hNSC secreting aaTSP-1 were shown by dual *in vitro* bioluminescence imaging (Fig. 3D). When a mix of glioma cells and hNSC co-expressing GFP-Fluc and aaTSP-1-Gluc was implanted subcutaneously in mice, dual bioluminescence imaging showed that aaTSP-1 expression could be measured *in vivo* and that the expression of aaTSP-1 *in vivo* was stable over time (Fig. 3E). In order to simultaneously follow tumor volumes, secretion of aaTSP-1 and localization of tumor cells and hNSC at a cellular resolution, we implanted hNSC-aaTSP-1-Gluc cells into mice with established Gli36-EGFRvIII-FD tumors, 2 mm from the site of implantation, in subcutaneous window chambers. Dual bioluminescence imaging revealed that the tumor volumes (Fig. 3F and 3H) and aaTSP-1 secretion (Fig. 3G and 3H) could be sequentially detected, and subsequent intravital microscopy on the same mice revealed the homing of NSC secreting aaTSP-1-Gluc to tumor cells (Fig. 3I–N) at a cellular resolution in real-time. These results reveal that that tumor volumes, anti-angiogenic agents and the delivery vehicles can be monitored longitudinally in real-time *in vivo* and further demonstrate that aaTSP-1 secretion from NSC is stable *in vivo* and engineered hNSC home to tumors.

To assess the effects of aaTSP-1 delivered via engineered hNSC on gliomas *in vivo*, we first implanted a mix of human Gli36-EGFRvIII-FD glioma cells and either aaTSP-1 expressing or control GFP-Rluc expressing hNSC. The presence of hNSC (green) within the implanted tumors (red) was confirmed by intravital microscopy 4 days post implantation (Fig. 4A). Serial Fluc bioluminescence imaging on mice revealed a significant reduction in glioma burden in animals bearing hNSC expressing aaTSP-1 as compared to the hNSC expressing control GFP-Rluc starting at day 6 post-implantation (Fig. 4A). Histopathological analysis with anti-CD31 antibody on tumor sections revealed that control tumor presented significantly higher number of vascular endothelial cells than treated tumors (Fig. 4B–D). In order to simultaneously follow tumor cells, NSC and tumor vasculature at a cellular resolution, we created a human malignant glioma cell line expressing a new red shifted marker, tdTomato, which is the brightest of the red shifted fluorophore variants (Gli36-EGFRvIII-tdTomato) (Fig. 4E) (1.6 times brighter than DsRed2; $t_{0.5}$ for maturation: 1 hr as compared to 7 hr for DsRed2) and implanted a mix of therapeutic hNSC-aaTSP-1 or control hNSC-GFP-Rluc and Gli36-EGFRvIII-tdTomato tumor cells in subcutaneous window chambers. Intravital confocal microscopy on mice 4 days after implantation revealed that tumor cells, hNSC and vasculature could be detected simultaneously (Fig. 4F–M) in both aaTSP-1 treated and control GFP-Rluc treated mice. Furthermore, a significant reduction in the microvascular density within the tumor mass was seen in aaTSP-1 treated tumors (Fig. 4J–M and Fig. 4N) as compared to the controls at day 6 post implantation (Fig. 4F–I and Fig. 4N). These experiments demonstrate that anti-angiogenic effects of aaTSP-1 have a substantial influence on the growth and progression of tumor cells in subcutaneous glioma tumors. Furthermore, using different combinations of optical imaging modalities, anti-angiogenic effects of hNSC delivered aaTSP-1 can be monitored in real-time *in vivo*.

Next, we tested the effect of hNSC-aaTSP-1 in the intracranial glioma models. Two different sets of experiments were performed. In the first set of experiments, we implanted a mix of hNSC-aaTSP-1 or control hNSC-GFP-Rluc and Gli36-EGFRvIII-tdtomato tumor cells in a cranial window model. Similar to the subcutaneous window chamber model, intravital confocal microscopy on mice revealed that tumor cells, hNSC and blood vasculature could be detected simultaneously in both control GFP-Rluc (Fig. 5A–D) and aaTSP-1 treated (Fig. 5E–H) mice. A considerable reduction in glioma volumes in tumors implanted with hNSC-aaTSP-1 (Fig. 5A) as compared to the controls (Fig. 5E) was observed 4 days after implantation. Furthermore, a significant reduction in vasculature around Gli36-EGFR-vIII-tdTomato/NSC-aaTSP-1 transplanted areas as compared to the controls (Fig. 5I).

A number of previous studies have revealed that repeated systemic administration of anti-angiogenic drugs in animal models result in controlled cell proliferation but incomplete eradication of established gliomas. In the second set of experiments, we assessed the effect of stem cell delivered aaTSP-1 on established gliomas by implanting hNSC-aaTSP-1 in the close vicinity to Gli36-EGFR-vIII-FD established gliomas. Dual bioluminescence imaging revealed the progression of glioma tumors (Fig. 5J) and fate of hNSC in real time (Fig. 5K). Glioma growth was significantly reduced at day 6, day 12 and day 16 after implantation compared to the control hNSC-GFP-Rluc implanted animals, where tumors grew more rapidly (Fig. 5J). Kaplan-Meier survival analysis revealed a statistically significant prolongation of the survival in the hNSC-aaTSP-1 treated group as compared to control hNSC-GFP-Rluc (Fig. 5l). Histological examination revealed prominent presence of endothelial cells in control tumors as compared to the aaTSP-1 tumors (Fig. 5M–O). These results show that a single administration of hNSC-aaTSP-1 in mice with established glioma result in significant reduction glioma growth and prolonged survival.

In order to investigate the fate of transplanted hNSC-aaTSP-1 in mice, immunohistochemical analysis on brain sections from mice bearing gliomas and implanted with hNSC-aaTSP-1 12 days post-implantation was performed. A robust expression of neural stem cell marker, nestin in hNSC 12 day post-implantation was observed (Fig. 6A–D). Furthermore a majority of hNSC-aaTSP-1 did not stain for the proliferation marker Ki67 (Fig. 6E–H), the astrocytic marker, GFAP (Fig. 6I–L) and the neuronal marker, MAP-2 (Fig. 6M–P) where as tumor cells were stained for Ki67 (Fig. 6E–H) and normal mouse brain stained for both GFAP (Fig. 6I–L) and MAP-2 (Fig. 6M–P). These results reveal that therapeutic hNSC do not proliferate and remain in an un-differentiated state in the brains of glioma bearing mice brains.

Discussion

In this study we have engineered and characterized a secretable form of anti-angiogenic TSP-1. We show that engineered hNSC expressing secretable aaTSP-1 have a significant anti-angiogenic effect on different endothelial cell types co-cultured with both established and primary glioma cells. Employing various fluorescence and bioluminescent proteins in combination with different optical imaging techniques, we show that hNSC- aaTSP-1 targets the vascular-component of gliomas. Furthermore, a single administration of NSC-aaTSP-1 markedly reduces tumor vessel-density that results in inhibition of tumor-progression and increased survival in mice.

Human glioblastomas are richly vascularized tumors (Zagzag et al., 2000) that actively release a substantial amount of stimulating factors and promote angiogenesis either by direct interaction with endothelial cells or by secretion of a large number of factors (Guerin & Laterra, 1997). In our co-culture experiments of endothelial cells with glioma cells, the

secreted aaTSP-1 was able to overcome the support of co-cultured glioma cells on endothelial cells, which use complex mechanisms to promote angiogenesis in their vicinity (Bergers & Benjamin, 2003; Jain et al., 2007). It has been shown that CD133+ brain cancer stem cells interact physically with endothelial cells in culture, in contrary to CD133− cells. They promote microvascular angiogenesis and are maintained in an undifferentiated state due to secreted factors from endothelial cells from their 'vascular niche' (Calabrese et al., 2007). In this study, we show that the presence of secreted aaTSP-1 in the medium of human brain endothelial cells in co-culture with both isolated CD133+ cancer stem cells and CD133− cells from a resected human primary brain tumor have a similar effect. These results reveal that glioma cells, irrespective of having cancer stem cell like properties, demonstrate similar sensitivity to the anti-angiogenic effect of aaTSP-1. The depletion of brain tumor vasculature by secreted aaTSP-1 could possibly destroy the vascular niche necessary for CD133+ cancer stem cell survival. These results confirm that aaTSP-1 is a potent inhibitor of endothelial cell migration and tubule formation induced by angiogenesis promoting factors secreted by tumor cells and present in the Matrigel basement membrane matrix.

Sustained levels of angiogenic inhibitors including 3TSR are a potential key to improving the efficiency and potency of anti-angiogenic cancer therapy (Batchelor et al., 2007; Capillo et al., 2003; Drixler et al., 2000; Kisker et al., 2001). The ability of the TSP-1 type 1 repeats to target endothelial cells makes it an attractive candidate for anti-angiogenic therapy in cancer treatment. However, the short blood circulating half-life of 3TSR(Hanahan & Weinberg, 2000) is a limitation to maintaining stable systemic levels of aaTSP-1. Recent studies have shown that *in vivo* continuous administration of the 3TSRs through mini-osmotic pump improves the potency of antiangiogenic therapy in an orthotopic human cancer model compared to repeated bolus administration (Zhang et al., 2007). Also, the results of a phase I clinical trial of ABT-510, a peptide derived from TSRs (Hoekstra et al., 2006), have further emphasized the need for continuous administration of peptides for anti-angiogenic therapy. In this study, we have engineered lentiviral vectors, that allow stable integration of transgenes into the host genome (Naldini et al., 1996), to express a smaller region of TSR, comprising of the whole of 2^{nd} TSR and parts of the 1^{st} and the 3^{rd} TSR fused to the N-terminal hFLt3 signal sequence. Utilizing the tumor homing properties of human NSC (Corsten & Shah, 2008; Shah et al., 2005; Tang et al., 2003), our studies show a sustained and continuous hNSC-mediated delivery of aaTSP-1 for at least 2 weeks post-implantation of hNSC.

Our *in vivo* results demonstrate that hNSC secreting aaTSP-1 within the tumors resulted in a significant reduction in tumor microvascular density. Secreted aaTSP-1 also exerted powerful anti- -growth effects on non-established tumor in the subcutaneously implanted model. This is most likely due to the continuous secretion of aaTSP-1 by hNSC in close proximity to the tumor cells which ensure effective local concentration of the anti-angiogenic protein *in vivo*. Later experiments, utilizing established glioma xenograft implanted intracranially followed by injection of aaTSP-1 expressing hNSC, also demonstrated reduction of tumor size and microvessel density up to day 16 post- hNSC implantation. This is in line with other studies which have revealed that anti-angiogenic therapies in animal models of glioma do not result in complete eradication of established gliomas but provide evidence of controlled cell proliferation (Tuettenberg et al., 2006). Recent studies have shown that the use of anti-angiogenic drugs in human brain tumor patients normalize the abnormal structure and function of the blood vessels, rendering them more efficient for the delivery of other therapeutic agents (Batchelor et al., 2007; Duda et al., 2007; Jain et al., 2007). Based on these studies, NSC expressing both aaTSP-1 and tumor specific cytotoxic agents, like S-TRAIL, (Shah et al., 2005; Shah et al., 2004; Sasportas et al., 2009) can be engineered and the efficacy of this stem cell based combination therapy can

be tested in pre-clinical trials. The onsite delivery of therapeutic agents via stem cells to target both brain tumor cells and tumor associated endothelial cells should allow for higher treatment efficiency and possibly for eradication of established gliomas.

The limited availability of noninvasive methods to monitor multiple molecular events has been one of the main limitations in testing the efficacy of various tumor therapy paradigms. In our previous studies, we have shown that we can follow delivery of viruses (Shah et al., 2003), neural stem cells (Shah et al., 2005) and quantify glioma burden *in vivo* (Kock et al., 2007; Shah et al., 2005; Shah et al., 2003) using non-invasive bioluminescence imaging. Despite the advantages and convenience of bioluminescence imaging for monitoring tumor growth, there are some disadvantages which should be taken into account while assessing fate of tumors and stem cells *in vivo*. The light transmission is attenuated by tissue, therefore deeper the luciferase expressing cells within the body or intracranial tumors, the greater the signal attenuation. In our studies on fate of NSCs in intracranial gliomas described in Fig. 5, we show that as the tumor size (Fluc activity) increases, there is a considerable decreases in NSCs (Rluc activity) over 2 weeks. As the decrease is seen only at the BLI level and not in tissue sections described in Fig. 6, we believe that as the tumors grow, they shield NSC which then become almost undetectable by bioluminescence imaging by week 2. In addition, while bioluminescence imaging is an efficient method for longitudinal imaging and confocal intravital microscopy offers great potential to image multiple events in real time. In the current studies, we have labeled tumor cells and stem cells with bimodal imaging markers (bioluminescent and fluorescent) expressed as a single transcript, which allows for expanding the number of events that can be visualized in real-time *in vivo*. To follow pharmacokinetics of therapeutic aaTSP-1 both in culture and in mouse models of glioma, we have also employed a C-terminal fusion of aaTSP-1 with Gluc, which is a relatively new bioluminescent protein that has been proven to optimized brightness and stability over other luciferases. (Verhaegent & Christopoulos, 2002). Although Gluc fusion reduced the anti-angiogenic activity of aaTSP-1, it was shown to be an efficient tool for real-time quantification of secreted aaTSP-1 *in vivo*. In addition, we have also used a blood pool agent, angiosense-750, to visualize the vasculature in the tumor area and the microvascular density within the tumors, by looking in dorsal skin-fold and intracranial window preparations which have been previously shown to facilitate the real-time analysis of angiogenesis and microcirculationin the tumors (Gondi et al., 2004). Previous intravital microscopy data indicated that the blood half-life of angiosense-750 is more than 5 hours, with essentially no extravasation into tumors during the first 30 minutes after intravenous administration (Montet et al., 2007).

In conclusion, this study simultaneously sheds light on the pharmacokinetics of secreted therapeutic proteins, fate of stem cells, tumor volumes and microvascular density and has implications in developing novel stem cell based therapies for cancer.

Materials and Methods

Generation of TSP-1 lentiviral vectors

Lentiviral vectors, pLV CSC-IG bearing an IRES-GFP (Internal ribosomal entry site-green fluorescent protein) element, were used as a backbone. The detailed construction of the therapeutic and diagnostic lentiviral vectors in this study is described in the Supplementary Methods section.

Cell Lines and Cell Culture

Human Gli36 and Gli36-EGFRvIII and Gli36-EGFRvIII line expressing Fluc-DsRed2 (Gli36-EGFRvIII-FD) human glioma cells and 293T/17 cells were grown as described

previously (Shah et al., 2005). Human Neural Stem Cells (hNSC, Kindly provided by Dr. Alberto Martinez Serrano, University of Madrid, Spain) were grown as described previously (Shah et al., 2008). Human microvascular endothelial cells (HMVECS) and human brain microvascular endothelial cells (HBMVECs) (Cambrex, East Rutherford, NJ) were grown as described in the Supplementary Methods section. Primary human CD133 positive and negative glioma cells were kindly provided by Hiroaki Wakimoto (MGH, Boston).

Lentiviral transductions and stable cell lines

hNSC were transduced with LV bearing different variants of aaTSP-1 or control LV bearing GFP-Fluc or GFP-Rluc at M.O.I =2 in a growth medium containing 4 μg/ml protamine sulfate (Sigma) and cells were visualized for GFP expression by fluorescence microscopy. Similarly, Gli36-EGFRvIII glioma cells were transduced with LV-tdTomato at M.O.I =2 and visualized for tdTomato expression. Following expansion in culture, both hNSC and glioma cells were sorted by fluorescence activated cell sorting (FACSAria Cell-Sorting System, BD Biosciences, San Jose, CA). Two week post-sort, cells were analyzed by flow cytometry (FACScalibur, BD Biosciences).

Western blot and dot blot analysis and ELISAs

The details on Western blot analysis on cell lysates and dot blot analysis and ELISA on conditioned culture medium is described in detail in the supplementary Methods section.

Matrigel assay

HMVECs and HBMEVCs were grown as described above. Eighty percent confluent 10-cm dishes of transduced hNSC were washed with PBS and incubated in10 mL hNSC growth medium for 24 h. Conditioned media was collected and centrifuged at 1,000 rpm. Endothelial cells were plated on Matrigel (Chemicon, Temecula, CA) and 24 hrs later LV transduced hNSC conditioned medium was added to Matrigel. Eighteen or 24 hrs later, photomicrographs were taken using the Nikon E400 light microscope (Nikon Instruments Inc, Melville, NY). Endothelial cell branch points and tubule length was assessed and averaged on each of the photomicrograph (n=6). Co-culture experiments were performed by simultaneously plating HMVECs and glioma cells on 20 μl of Matrigel in 96 well plates and 18 hrs later incubating cells with NSC conditioned medium, followed by imaging on the next day. HMVECs co-cultured with Gli36vIII-DsRed2 were incubated in a medium containing different concentrations (0.1- 1 μM) of VEGFR2 kinase inhibitor 1 (Z)-3- [(2,4-Dimethyl-3- (ethoxy carbonyl)pyrrol-5-yl)methylidenyl]indolin-2-1 (Calbiochem) and 18 hrs later branch-points were measured as described above.

Pharmacokinetic assays

The *in vitro* dual-bioluminescence assays are described in the Supplementary Methods section. For in vivo pharmacokinetics, SCID mice (SCID; 3 weeks of age; Charles River Laboratories, Wilmington, MA, USA) were anesthetized by isofluorine inhalation. Two different sets of experiments were performed: 1) hNSC expressing aaTSP-1-Gluc and GFP-Fluc and Gli36-EGFRvIII cells were harvested by trypsinization. A mix of 3×10^6 hNSC-aaTSP-1-Gluc/GFP-Fluc and 3×10^6 Gli36-EGFR-vIII were implanted subcutaneously in SCID mice (n=4). Dual bioluminescence imaging in vivo was performed as described previously (Sasportas et al., 2009); 2) Gli36-EGFRvIII-FD glioma cells (3×10^6) were placed in the upper tissue layer of the center of the dorsal skin fold-window that were created as described previously (Asaishi et al., 1981; Carmeliet & Jain, 2000) (n=6) and four days later, hNSC expressing aaTSP-1-Gluc (1×10^6) were placed around the tumor cells. Mice were sequentially imaged for dual luciferase imaging as described previously (Sasportas et

al., 2009). Intravital fluorescence microscopy was performed as described in the Supplementary Methods section.

Tumor progression bioluminescence imaging

in vivo: Gli36-EGFRvIII-FD and human neural stem cells expressing aaTSP-1 or GFP-Rluc were harvested at 80% confluency and a mix of glioma cells (5×10^6) and transduced hNSC (2.5×10^6) (n= 4 mice in each case; 2 implantations/mouse) was injected subcutaneously in isofluorine anesthetized SCID mice. To follow the progression of glioma cells in a subcutaneous tumor model, mice were imaged for Fluc activity on day 1, 6, 10 and 14 as described previously (Sasportas et al., 2009). On day 15, mice were sacrificed and the subcutaneous tumors were resurrected for histopathological analysis. For intravital microscopy in subcutaneous tumor models, dorsal skin fold-window was created as described above. A mix of Gli36-vIII-tdtomato glioma cells (1×10^6) and hNSC-aaTSP-1 or hNSC-GFP-Rluc (1×10^6) (n=6 in each case) were placed on the upper tissue layer in the center of skin window. Four days post implantation, mice were injected with Angiosense-750 (Visen Medical, Woburn MA; 20 nmol/mouse) intravenously and intravital microscopy was performed as described in the Supplementary Methods section. Quantitative vascular analysis was performed by determination of micro vascular density (MVD), which was defined as the intensity of all newly formed microvesselsin five randomized areas within the tumors.

To follow the effect of hNSC secreting TSP-1 on growth of established gliomas in the brain, Gli36-EGFRvIII-FD glioma cells were harvested by trypsinization and implanted into right frontal lobe of SCID mice brains (80,000 cells/mouse, in 4μl PBS, n=10) (from bregma, AP: −2 mm, ML: 1.5 mm V (from dura): 2 mm). Three days after glioma cell implantations, mice were imaged for Fluc activity before their distribution into two experimental groups. hNSC expressing aaTSP-1 or GFP-Rluc only were harvested and implanted stereotactically (0.5×10^6 in 5ul PBS) (from bregma, AP: −2 mm, ML: 1.0 mm V (from dura): 2 mm, n=5 in each case). Mice were imaged sequentially for Fluc and Rluc activity starting day 3 as described previously (Sasportas et al., 2009). On day 16, mice were sacrificed and glioma tumors were resected for histopathological analysis. For intravital microscopy (described in detail in Supplementary Methods section), a small circular portion of the cortical surface was exposed and a mix of tdTomato glioma cells (200,000 cells/mouse) and hNSC either expressing aaTSP-1 or GFP-Rluc (200,000 cells/mouse) glioma cells were implanted stereotactically (from bregma, AP: -2 mm, ML: 1.5 mm V (from dura): 2 mm) (n=3 in each case). Mice were injected intravenously with Angiosense-750 (Visen Medical, Woburn MA; 20 nmol/mouse) and intravital microscopy was performed.

Tissue processing and immunohistochemisty

Immediately following the last imaging session, mice were perfused by pumping ice-cold 4% PFA directly into the heart for 5 min and prepared for immunohistochemistry, the details of which are described in the Supplementary Methods section.

Statistical analysis

Data were analyzed by Student t test when comparing 2 groups and by ANOVA, followed by Dunnetts post-test when comparing greater than 2 groups. Data were expressed as mean ±SEM and differences were considered significant at $P<0.05$. Survival times of the mouse groups treated with hNSC-aaTSP-1 and hNSC-GFP-Rluc were compared using log-rank tests.

Supplementary Material

Refer to Web version on PubMed Central for supplementary material.

Acknowledgments

This work was supported by American Brain Tumor Association grant (KS), Goldhirsh foundation (KS), Pappas foundation (KS), P50 CA86355 (RW), R21 (KS). We would like to Dr. Rainer Koehler with his help with intravital microscopy and Dr. Claudio Vinegoni for his help with processing images. We would also like to thank Maarten Corsten and Dr. Paul van Bergen en Henegouwen (Utrecht University, The Netherlands) for their constructive comments.

References

Aboody KS, Brown A, Rainov NG, Bower KA, Liu S, Yang W, Small JE, Herrlinger U, Ourednik V, Black PM, Breakefield XO, Snyder EY. Tumor progression: the effects of thrombospondin-1 and -2. Int J Biochem Cell Biol Proc Natl Acad Sci U S A. 2000; 97:12846–51.

Anderson JC, Grammer JR, Wang W, Nabors LB, Henkin J, Stewart JE Jr, Gladson CL. ABT-510, a modified type 1 repeat peptide of thrombospondin, inhibits malignant glioma growth in vivo by inhibiting angiogenesis. Cancer Biol Ther. 2007; 6:454–62. [PubMed: 17384534]

Asaishi K, Endrich B, Gotz A, Messmer K. Quantitative analysis of microvascular structure and function in the amelanotic melanoma A-Mel-3. Cancer Res. 1981; 41:1898–904. [PubMed: 7214358]

Batchelor TT, Sorensen AG, di Tomaso E, Zhang WT, Duda DG, Cohen KS, Kozak KR, Cahill DP, Chen PJ, Zhu M, Ancukiewicz M, Mrugala MM, Plotkin S, Drappatz J, Louis DN, Ivy P, Scadden DT, Benner T, Loeffler JS, Wen PY, Jain RK. AZD2171, a pan-VEGF receptor tyrosine kinase inhibitor, normalizes tumor vasculature and alleviates edema in glioblastoma patients. Cancer Cell. 2007; 11:83–95. [PubMed: 17222792]

Bergers G, Benjamin LE. Tumorigenesis and the angiogenic switch. Nat Rev Cancer. 2003; 3:401–10. [PubMed: 12778130]

Bogdanov A Jr, Marecos E, Cheng HC, Chandrasekaran L, Krutzsch HC, Roberts DD, Weissleder R. Treatment of experimental brain tumors with trombospondin-1 derived peptides: an in vivo imaging study. Neoplasia. 1999; 1:438–45. [PubMed: 10933059]

Calabrese C, Poppleton H, Kocak M, Hogg TL, Fuller C, Hamner B, Oh EY, Gaber MW, Finklestein D, Allen M, Frank A, Bayazitov IT, Zakharenko SS, Gajjar A, Davidoff A, Gilbertson RJ. A perivascular niche for brain tumor stem cells. Cancer Cell. 2007; 11:69–82. [PubMed: 17222791]

Capillo M, Mancuso P, Gobbi A, Monestiroli S, Pruneri G, Dell'Agnola C, Martinelli G, Shultz L, Bertolini F. Continuous infusion of endostatin inhibits differentiation, mobilization, and clonogenic potential of endothelial cell progenitors. Clin Cancer Res. 2003; 9:377–82. [PubMed: 12538491]

Carmeliet P, Jain RK. Angiogenesis in cancer and other diseases. Nature. 2000; 407:249–57. [PubMed: 11001068]

Corsten MF, Shah K. Therapeutic stem-cells for cancer treatment: hopes and hurdles in tactical warfare. Lancet Oncol. 2008; 9:376–84. [PubMed: 18374291]

Drixler TA, Borel Rinkes IH, Ritchie ED, van Vroonhoven TJ, Gebbink MF, Voest EE. Continuous administration of angiostatin inhibits accelerated growth of colorectal liver metastases after partial hepatectomy. Cancer Res. 2000; 60:1761–5. [PubMed: 10749151]

Duda DG, Batchelor TT, Willett CG, Jain RK. VEGF-targeted cancer therapy strategies: current progress, hurdles and future prospects. Trends Mol Med. 2007; 13:223–30. [PubMed: 17462954]

Ehtesham M, Kabos P, Gutierrez MA, Chung NH, Griffith TS, Black KL, Yu JS. Induction of glioblastoma apoptosis using neural stem cell-mediated delivery of tumor necrosis factor-related apoptosis-inducing ligand. Cancer Res. 2002; 62:7170–4. [PubMed: 12499252]

Gondi CS, Lakka SS, Dinh DH, Olivero WC, Gujrati M, Rao JS. Downregulation of uPA, uPAR and MMP-9 using small, interfering, hairpin RNA (siRNA) inhibits glioma cell invasion, angiogenesis and tumor growth. Neuron Glia Biol. 2004; 1:165–176. [PubMed: 16804563]

Guerin C, Laterra J. Regulation of angiogenesis in malignant gliomas. Exs. 1997; 79:47–64. [PubMed: 9002220]

Hanahan D, Weinberg RA. The hallmarks of cancer. Cell. 2000; 100:57–70. [PubMed: 10647931]

Hoekstra R, de Vos FY, Eskens FA, de Vries EG, Uges DR, Knight R, Carr RA, Humerickhouse R, Verweij J, Gietema JA. Phase I study of the thrombospondin-1-mimetic angiogenesis inhibitor ABT-510 with 5-fluorouracil and leucovorin: a safe combination. Eur J Cancer. 2006; 42:467–72. [PubMed: 16406507]

Jain RK, di Tomaso E, Duda DG, Loeffler JS, Sorensen AG, Batchelor TT. Angiogenesis in brain tumors. Nat Rev Neurosci. 2007; 8:610–22. [PubMed: 17643088]

Kisker O, Becker CM, Prox D, Fannon M, D'Amato R, Flynn E, Fogler WE, Sim BK, Allred EN, Pirie-Shepherd SR, Folkman J. Continuous administration of endostatin by intraperitoneally implanted osmotic pump improves the efficacy and potency of therapy in a mouse xenograft tumor model. Cancer Res. 2001; 61:7669–74. [PubMed: 11606410]

Kock N, Kasmieh R, Weissleder R, Shah K. Tumor therapy mediated by lentiviral expression of shBcl-2 and S-TRAIL. Neoplasia. 2007; 9:435–42. [PubMed: 17534449]

Lawler J, Detmar M. Int J Biochem Cell Biol. 2004; 36:1038–45. [PubMed: 15094119]

Liu P, Wang Y, Li YH, Yang C, Zhou YL, Li B, Lu SH, Yang RC, Cai YL, Tobelem G, Caen J, Han ZC. Adenovirus-mediated gene therapy with an antiangiogenic fragment of thrombospondin-1 inhibits human leukemia xenograft growth in nude mice. Leuk Res. 2003; 27:701–8. [PubMed: 12801528]

Markovic SN, Suman VJ, Rao RA, Ingle JN, Kaur JS, Erickson LA, Pitot HC, Croghan GA, McWilliams RR, Merchan J, Kottschade LA, Nevala WK, Uhl CB, Allred J, Creagan ET. A phase II study of ABT-510 (thrombospondin-1 analog) for the treatment of metastatic melanoma. Am J Clin Oncol. 2007; 30:303–9. [PubMed: 17551310]

Montet X, Figueiredo JL, Alencar H, Ntziachristos V, Mahmood U, Weissleder R. Tomographic fluorescence imaging of tumor vascular volume in mice. Radiology. 2007; 242:751–8. [PubMed: 17325064]

Naldini L, Blomer U, Gage FH, Trono D, Verma IM. Efficient transfer, integration, and sustained long-term expression of the transgene in adult rat brains injected with a lentiviral vector. Proc Natl Acad Sci U S A. 1996; 93:11382–8. [PubMed: 8876144]

Papetti M, Herman IM. Mechanisms of normal and tumor-derived angiogenesis. Am J Physiol Cell Physiol. 2002; 282:C947–70. [PubMed: 11940508]

Rusk A, McKeegan E, Haviv F, Majest S, Henkin J, Khanna C. Preclinical evaluation of antiangiogenic thrombospondin-1 peptide mimetics, ABT-526 and ABT-510, in companion dogs with naturally occurring cancers. Clin Cancer Res. 2006; 12:7444–55. [PubMed: 17189418]

Sasportas LS, Kasmieh R, Wakimoto H, Hingtgen S, van de Water JA, Mohapatra G, Figueiredo JL, Martuza RL, Weissleder R, Shah K. Assessment of therapeutic efficacy and fate of engineered human mesenchymal stem cells for cancer therapy. Proc Natl Acad Sci U S A. 2009; 106:4822–7. [PubMed: 19264968]

Shah K, Bureau E, Kim DE, Yang K, Tang Y, Weissleder R, Breakefield XO. Ann Neurol. 2005; 57:34–41. [PubMed: 15622535]

Shah K, Hingtgen S, Kasmieh R, Figueiredo JL, Garcia-Garcia E, Martinez-Serrano A, Breakefield X, Weissleder R. Bimodal viral vectors and in vivo imaging reveal the fate of human neural stem cells in experimental glioma model. J Neurosci. 2008; 28:4406–13. [PubMed: 18434519]

Shah K, Tang Y, Breakefield X, Weissleder R. Real-time imaging of TRAIL-induced apoptosis of glioma tumors in vivo. Oncogene. 2003; 22:6865–72. [PubMed: 14534533]

Shah K, Tung CH, Yang K, Weissleder R, Breakefield XO. Inducible release of TRAIL fusion proteins from a proapoptotic form for tumor therapy. Cancer Res. 2004; 64:3236–42. [PubMed: 15126365]

Tang Y, Shah K, Messerli SM, Snyder E, Breakefield X, Weissleder R. In vivo tracking of neural progenitor cell migration to glioblastomas. Hum Gene Ther. 2003; 14:1247–54. [PubMed: 12952596]

Tuettenberg J, Friedel C, Vajkoczy P. Angiogenesis in malignant glioma--a target for antitumor therapy? Crit Rev Oncol Hematol. 2006; 59:181–93. [PubMed: 16860996]

Verhaegent M, Christopoulos TK. Recombinant Gaussia luciferase. Overexpression, purification, and analytical application of a bioluminescent reporter for DNA hybridization. Anal Chem. 2002; 74:4378–85. [PubMed: 12236345]

Zagzag D, Amirnovin R, Greco MA, Yee H, Holash J, Wiegand SJ, Zabski S, Yancopoulos GD, Grumet M. Vascular apoptosis and involution in gliomas precede neovascularization: a novel concept for glioma growth and angiogenesis. Lab Invest. 2000; 80:837–49. [PubMed: 10879735]

Zhang X, Connolly C, Duquette M, Lawler J, Parangi S. Continuous administration of the three thrombospondin-1 type 1 repeats recombinant protein improves the potency of therapy in an orthotopic human pancreatic cancer model. Cancer Lett. 2007; 247:143–9. [PubMed: 16757110]

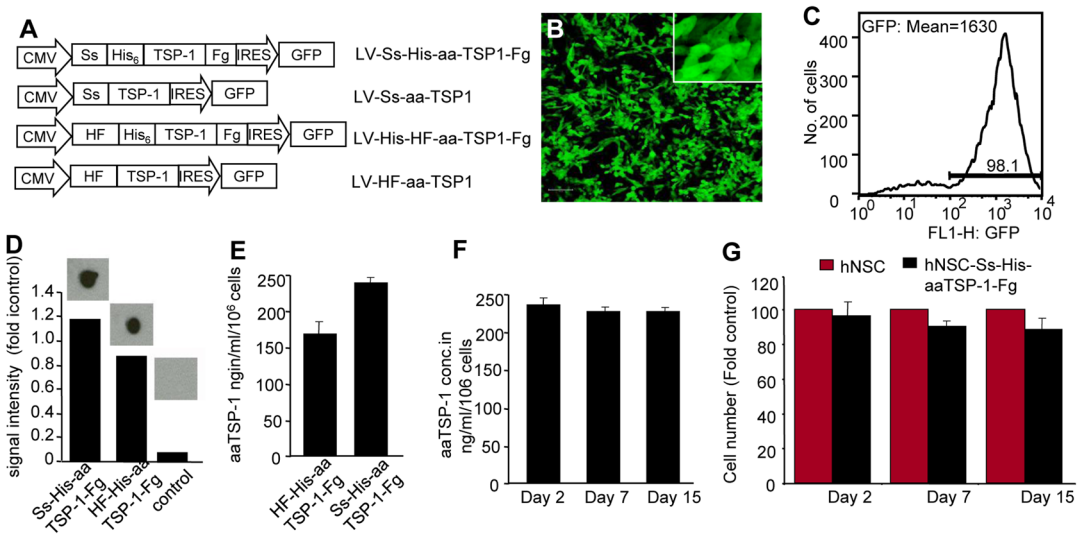

Fig. 1. Characterization of aaTSP-1 lentiviral vectors

(A) Design of lentiviral vectors (LV) expressing different variants of aaTSP-1. The cDNAs were cloned in front of the cytomegalovirus (CMV) promoter in LV-CSCIG which bears an internal ribosomal entry site (IRES) and GFP. (B) Representative GFP fluorescence image of hNSC transduced with LV bearing different variants of aaTSP-1. (C) FACS analysis of sorted GFP positive cells expressing aaTSP-1. (D) Dot blot analysis on His-aaTSP-1-Fg secreted in the culture medium. (E–F) ELISA on His_6 and FLAG tagged aaTSP-1 expressing hNSC culture medium showing the concentration of aaTSP-1 secreted by hNSC expressing different variants of aaTSP-1 and Ss-His-aaTSP-1-Fg overtime. (G) Cell viability of hNSC expressing Ss-His-aaTSP-1-Fg and non-transduced hNSC over 15 days. Magnification B (10×); inset (40×).

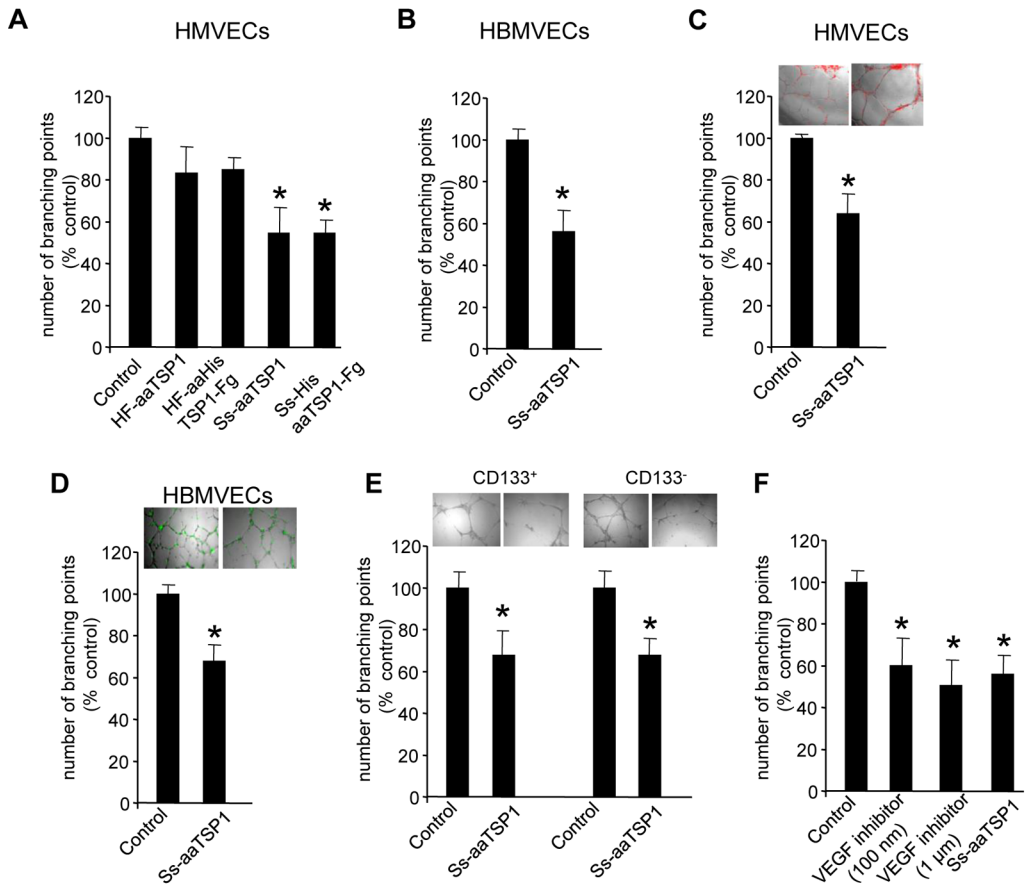

Fig. 2. aaTSP-1 has anti-angiogenic effect on human endothelial cells

(A) HMVEC were incubated in conditioned medium from transduced hNSC expressing control GFP-Rluc, Ss-aaTSP-1, HF-aaTSP-1, Ss-His-aaTSP-1-Fg or HF-His-aaTSP-1-Fg and 18 hrs later branch-points were measured. (B) HBMVECs were incubated in conditioned medium from transduced hNSC expressing control GFP-Rluc or Ss-aaTSP-1, and 18 hrs later branch-points were measured. (C and D) Photomicrographs and average branch points of HMVECs (C) and HBMVECs (D) co-cultured with Gli36-EGFRvIII-DsRed2 glioma cells and incubated with conditioned medium from hNSC-GFP-Rluc or hNSC-Ss-aaTSP-1. (E) HMVECs co-cultured with CD133+ and CD133- primary glioma cells were incubated in conditioned medium from hNSC-GFP-Rluc or hNSC-Ss-aaTSP-1 and 18 hrs later branch-points were measured. (F) HMVECs co-cultured with Gli36-EGFRvIII-DsRed2 glioma cells were incubated in conditioned medium from hNSC-GFP-Rluc or hNSC-Ss-aaTSP-1 or medium containing different concentrations of VEGFR inhibitors, and 18 hrs later branch-points were measured. *In all panels $p<0.03$ vs control. Data are mean ±SD (n=6) and expressed relative to control.

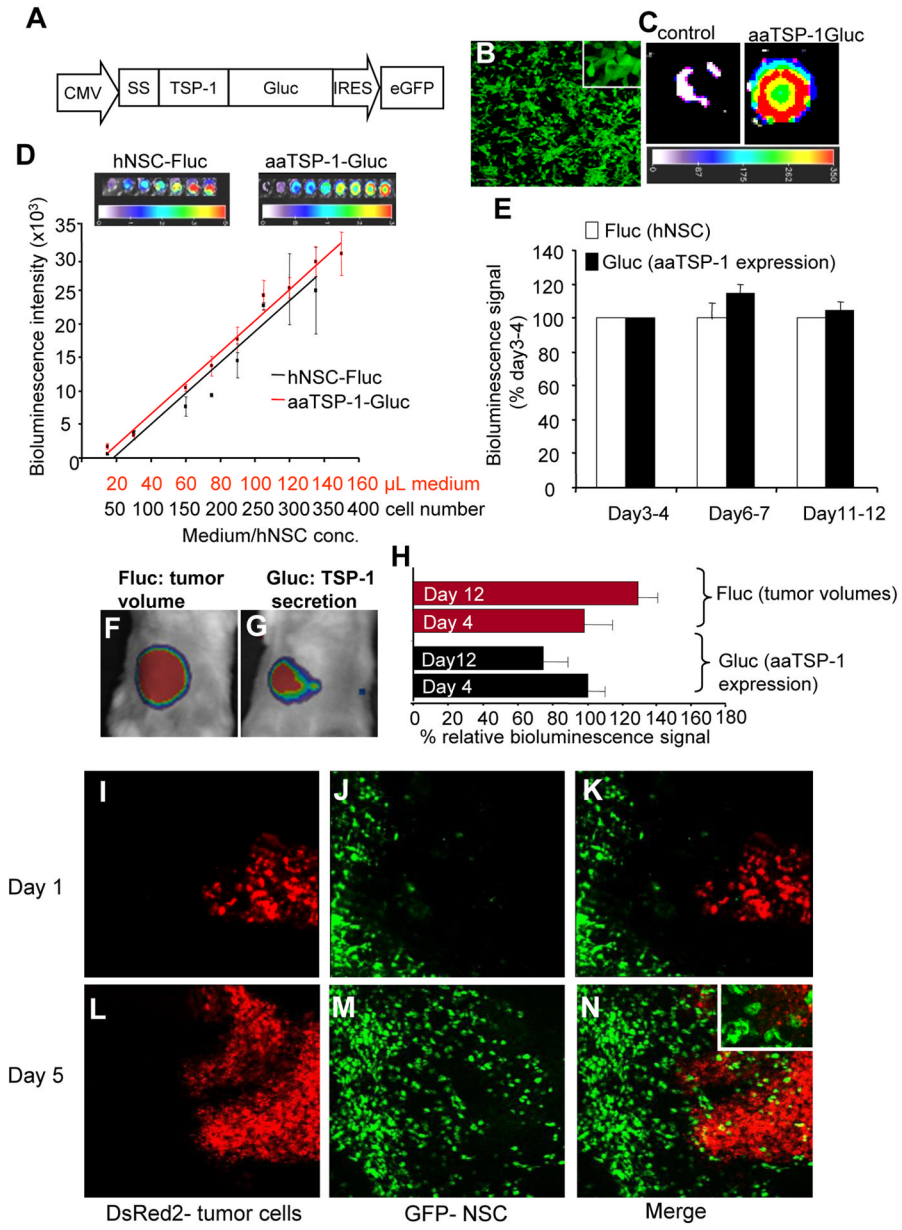

Fig. 3. Pharmacokinetics of hNSC-aaTSP1

(A) Design of LV-aaTSP-1-Gluc construct showing the C-terminal fusion of aaTSP-1 with *in vivo* imaging marker, Gluc. (B) GFP fluorescence image of hNSC transduced with LV-aaTSP-1-Gluc. (C) Bioluminescence imaging of the conditioned medium from hNSC-aaTSP-1-Gluc (D) hNSC expressing aaTSP-1-Gluc were co-transduced with GFP-Fluc and cells and conditioned culture medium were imaged for Fluc and Gluc activity respectively. Correlation between the different concentrations of cells-Fluc activity and medium-Gluc activity within the ranges tested are plotted. (E) hNSC expressing aaTSP-1-Gluc and GFP-Fluc were mixed with Gli36-EGFRvIII-DsRed2 glioma cells and implanted subcutaneously in nude mice and imaged sequentially for Fluc and Gluc activity. Plot showing bioluminescence signal (Fluc and Gluc) intensity of mice imaged for a period of 12 days. (F–J) Simultaneous dual bioluminescence imaging and intravital microscopy on mice implanted with hNSC-aa-TSP-1-Gluc at 2 mm distance from the established Gli36-

EGFRvIII-FD tumor site. Representative images of mice (F and G) and plot (H) showing the changes in tumor volumes (Fluc intensity) and aaTSP-1 secretion (Rluc intensity) overtime. (I–N) Intravital fluorescent images showing the homing of hNSC (GFP expression) to tumor cells (DsRed2 expression). Magnification I-N (10×); inset N (20×).

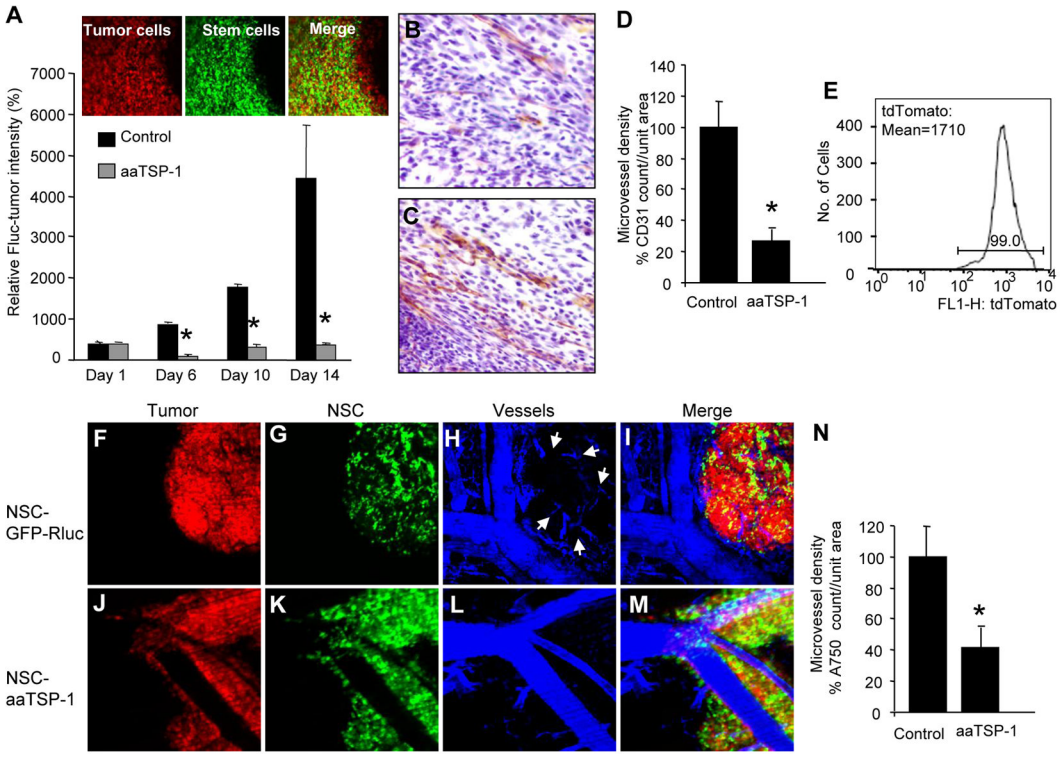

Fig. 4. NSC delivered aaTSP-1 influences tumor formation *in vivo*

Gli36-EGFRvIII-FD were mixed with hNSC-aaTSP-1 or hNSC-GFP-Rluc and implanted subcutaneously in nude SCID mice. (A) Mice were imaged for Fluc activity on day 1, 6, 10 and 14 and the relative Fluc intensities (tumor burden) are plotted. Representative intravital images showing the mix of tumor cells (red) and hNSC (green) within the tumor. (B–D) Immnohistochemical analysis of CD31 expression (microvessel density) in sections of glioma xenografts 14 days after implantation: aaTSP-1 (B) and control glioma sections (C). Graph depicting microvessel density in aaTSP-1 and control gliomas (D). (E) FACS analysis of sorted Gl36-EGFRvIII expressing tdTomato (F–M) Gli36vIII-tdTomato glioma cells were mixed with hNSC-aaTSP-1 or hNSC-GFP-Rluc and placed into dorsal skin fold-window chamber of nude SCID mice. Intravital fluorescent pictures of a day 4 control hNSC-GFP-Rluc (F–I) and hNSC-aaTSP-1 (J–M) tumor bearing mice are shown. (N) Graph depicting the intensity of angiosense-750 labeling (microvascular density) within the aaTSP-1 and control tumors. *In panels a, d and n, $p<0.05$ vs control. Data are mean ±SD (n=5) and expressed relative to control. Magnification B–C (20x), F–M (20×)

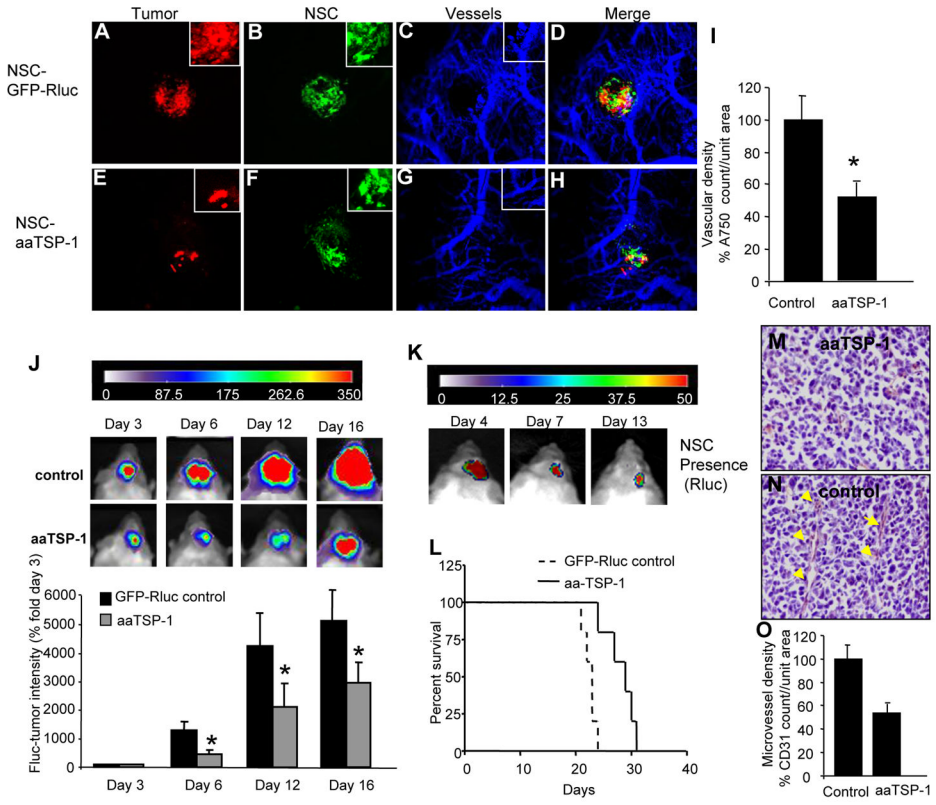

Fig. 5. NSC delivered aaTSP-1 has anti-proliferative effect on established intracranial gliomas

(A–H) Gli36vIII-tdTomato cells were mixed with hNSC-aaTSP-1 or hNSC-GFP-Rluc, implanted into the frontal lobe of nude SCID mice and 4 days later injected with Angiosense-750 intravenously. Intravital fluorescent pictures of a day 4 control hNSC-GFP-Rluc (A–D) and hNSC-aaTSP-1 (E–H) and glioma bearing brains are shown. (I) Graph depicting the intensity of angiosense-750 labeling (vasculature) around aaTSP1 and control tumors. (J–K) hNSC-aaTSP-1 and control hNSC-GFP-Rluc were implanted in the close vicinity of established Gli36-EGFRvIII-FD gliomas. Both aaTSP-1 treated and control mice were imaged for Fluc activity (glioma burden) on day 3, 6, 12 and 16 days post hNSC implantation. Relative Fluc intensities (glioma burden) are plotted (J). Mice bearing control GFP-Rluc hNSC were also imaged for Rluc activity (hNSC presence) on day 4, 7 and 13 days after implantation (K). (L) Survival curves of hNSC-aaTSP-1 and hNSC-GFP-Rluc treated mice (M–N) Representative images of brain sections immunostained for CD31. *In panels I, J and L, $p<0.05$ vs control. (O) Graph depicting microvessel density in aaTSP-1 and control gliomas. Data are mean ±SD and expressed relative to control.

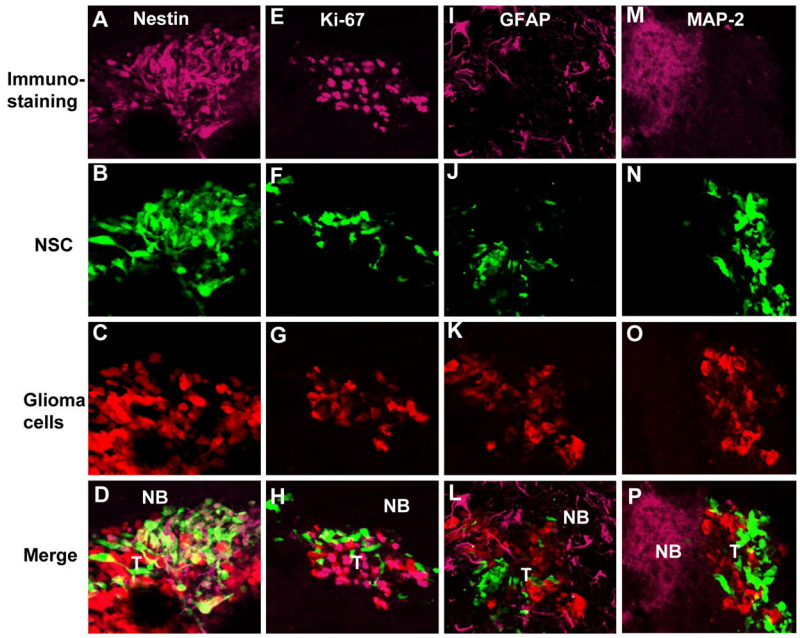

Fig. 6. Engineered hNSC do not differentiate in mouse glioma model

hNSC-aaTSP-1 or control hNSC-GFP-Rluc were implanted in the close vicinity of established Gli36-EGFRvIII-FD gliomas. Representative images of brain sections of hNSC-aaTSP-1 mice sacrificed on day 12 and immunostained with nestin, Ki67, GFAP and MAP-2 antibodies. Different panels showing the expression of tumor cells (red), hNSC (green) and nestin, Ki67, GFAP or MAP-2 immunostaining (purple). NB-normal brain; T-tumor.